

Effect of Oxide Species and Thermomechanical Treatments on the Strength Properties of Mechanically Alloyed Fe-17%Cr Ferritic ODS Materials

Ick-Soo Kim, Takanari Okuda*, Chang-Yong Kang**, Jang-Hyun Sung***

Philip J. Maziasz[†], Ronald L. Klueh[†] and Kazuya Miyahara^{††}

Graduate School, Naogya University, Nagoya 464-8603, Japan.

*Materials Research Institute, Kobe Steel Ltd., Kobe 651-2271, Japan

**Department of Materials Science and Engineering, Pukyong National University
San 100 Yongdang-dong, Nam-ku, Pusan 608-739, Korea

***Department of Metallurgical Engineering, Dong-A University
840 Hadan-dong, Saha-ku, Pusan 604-714, Korea.

[†]Metals and Ceramics Division, Oak Ridge National Laboratory, Oak Ridge, TN 37831-6115, USA

^{††}Department of Molecular Design and Engineering, Nagoya University, Nagoya 464-8603, Japan

The effects of several oxide species, such as Y_2O_3 , ZrO_2 and MgO , and the thermomechanical treatment (TMT) after the mechanical alloying (MA) process on the strength properties of Fe-17%Cr ferritic ODS (oxide dispersion strengthening) MA materials were investigated. Y_2O_3 showed the most uniform dispersion of the finest particles among the above oxides, but the microstructural evolution during the TMT had a larger effect on the strengthening of the alloys than the fine and uniform dispersion of the Y_2O_3 particles had.

Keywords : ferritic alloy, mechanical alloying oxide dispersion strengthening, ODS, yttria, zirconia, magnesia, high temperature strength, thermomechanical treatment

1. INTRODUCTION

Recently, the effects of oxide dispersoid species on the strength properties of Fe-17 to 20% Cr ferritic MA-ODS materials have been investigated by Kawasaki *et al.* [1] and the present authors [2]. Their results indicated that, in the case of the sole addition of Y_2O_3 , Al_2O_3 , TiO_2 , ZrO_2 , SiO_2 and MgO , the particles of Y_2O_3 were the finest and showed the most uniform size and space distribution among the above oxides and that the addition of Y_2O_3 was most effective in increasing the strength properties of the materials. As one example of oxide dispersion strengthening, the finest distribution of these uniform oxides operates powerfully upon strength characteristics by restraint for dislocation migration. It is well known that the finer the grains are and the shorter the distance between oxide particles are, the more the strength effect will increase. The present researchers [3] investigated the effect of distribution condition of oxide particles and TMT (thermomechanical treatment) on elevated temperature strength characteristics. This results showed that the TMT after MA (mechanical alloying) had a

more significant effect on strength properties of the materials than did the effect of the addition of oxides. This study clarifies the variation of strength characteristics by TMT after MA for the most suitable material designs of ODS alloys and the effect of their recrystallization behaviour.

2. EXPERIMENTAL PROCEDURES

The materials used in this research are produced by an MA followed by the TMT process. Raw metal powder with a particle size of about 100 mesh and Y_2O_3 , ZrO_2 and MgO powders were mechanically alloyed using a high energy attrition ball mill.

The mill charge was about 1kg of alloying powders with 15 kg steel balls of 9.5 in diameter. The powders were mixed for 48 hrs in an argon atmosphere (Argon gas pressure: 200 mmH₂O) at an agitator speed of 290 rpm. The mechanically alloyed powders were packed into a mild steel tube, hot-extruded to a bar (diameter: 30 mm) at temperatures from 1123 to 1323 K and hot-rolled into a plate (thickness: 7.0 mm) at temperatures from 1123 to

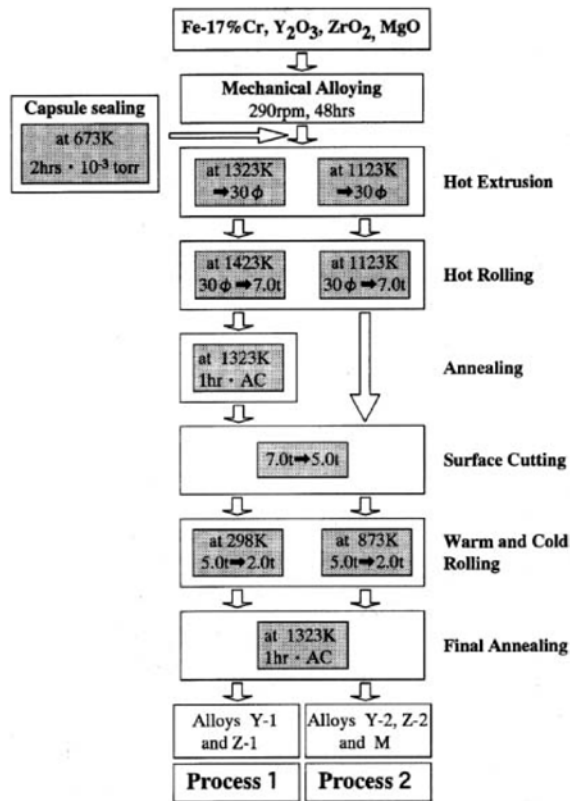


Fig. 1. Manufacturing process of the 17Cr ODS-MA ferritic alloys.

1423 K. The materials were cold rolled or warm rolled at 873 K. Finally, the materials were normalized at 1323 K for 1hr. A schematic diagram of these procedures is shown in Fig. 1. TMT after the MA process is categorized into two processes (processes 1 and 2). The chemical compositions of the materials are shown in Table 1. The added oxide content is a successful manufacturing process considering the optimum recrystallization region and strength mechanism [4]. After the final heat treatment, the materials were machined to flat tensile test specimens with a gauge length of 2.0 mm width, 2.0 mm thickness and 10.0 mm length.

Tensile tests were performed at temperatures from 298 to 1173 K and a strain rate of 8.3×10^{-4} /s using an Instron type testing machine. The microstructure of the materials was observed by OM (optical microscope) and TEM (transmission electron microscope).

3. EXPERIMENTAL RESULTS AND DISCUSSIONS

Fig. 2 shows the typical stress-strain curves of the materials obtained by a tensile test at 298 K. Temperature dependences of the tensile strength and elongation of the materials are shown in Fig. 3. This result indicates that the materials containing Y_2O_3 do not necessarily have the greatest tensile strength and that the TMT contributed more to the strengthening than the oxide species had. Generally, oxide dispersoid strengthening alloys are well known to increase strength because of the obstacle of dislocation migration shown in the Orowan model [5], cross slip model [6] and dislocation climb model [7], etc. The results from Fig. 3 as shown in Fig. 4 show that the strengths of 17Y-2, 17Z-2 and 17M produced by process 2 where higher in spite of Y_2O_3 having the finest

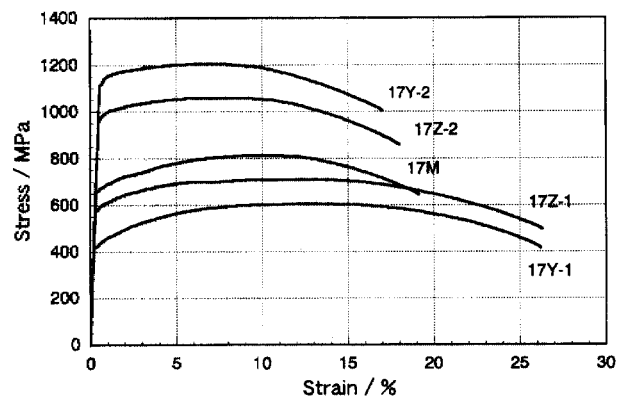


Fig. 2. Stress-strain curves obtained by the tensile test at 298K.

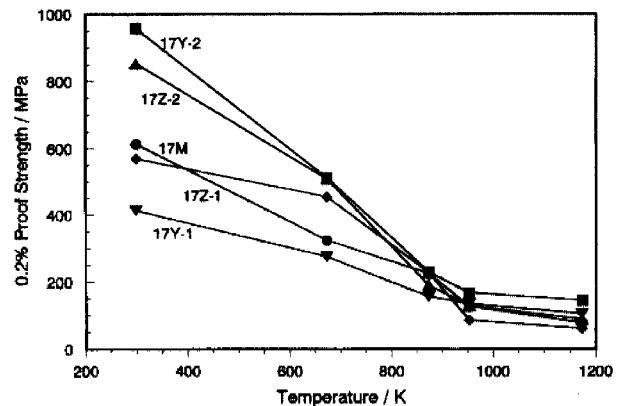


Fig. 3. Temperature dependence of 0.2% proof strength of the 17% Cr ODS-MA ferritic alloys.

Table 1. Chemical composition of the materials used (mass%)

| Materials | C | Cr | Y | Zr | Mg | O | N | Oxide |
|-----------------|-------|-------|------|------|------|------|--------|----------------|
| 17Y-1 and 17Y-2 | <0.05 | 16.25 | 0.19 | - | - | 0.12 | 0.097 | $Y_2O_3(0.24)$ |
| 17Z-1 and 17Z-2 | <0.05 | 15.96 | - | 0.14 | - | 0.14 | 0.095 | $ZrO_2(0.18)$ |
| 17M | <0.05 | 16.80 | - | - | 0.12 | 0.16 | 0.0086 | $MgO(0.20)$ |

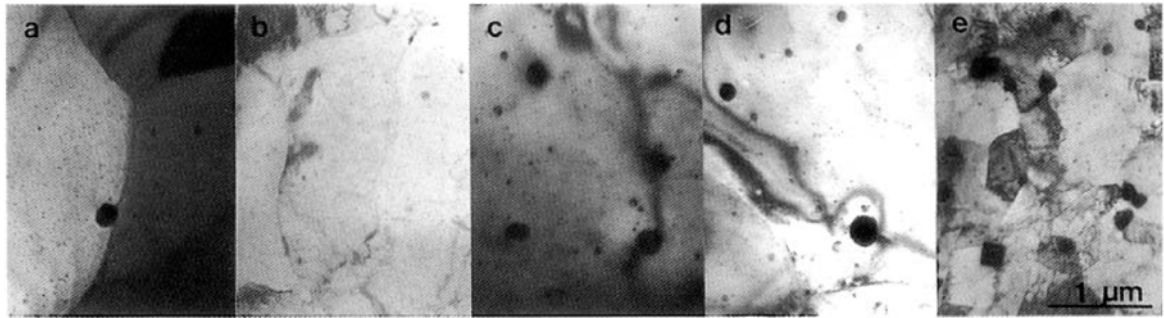


Fig. 4. Oxide particles distribution in the alloys. (a) 17Y-1, (b) 17Y-2, (c) 17Z-1, (d) 17Z-2, and (e) 17M.

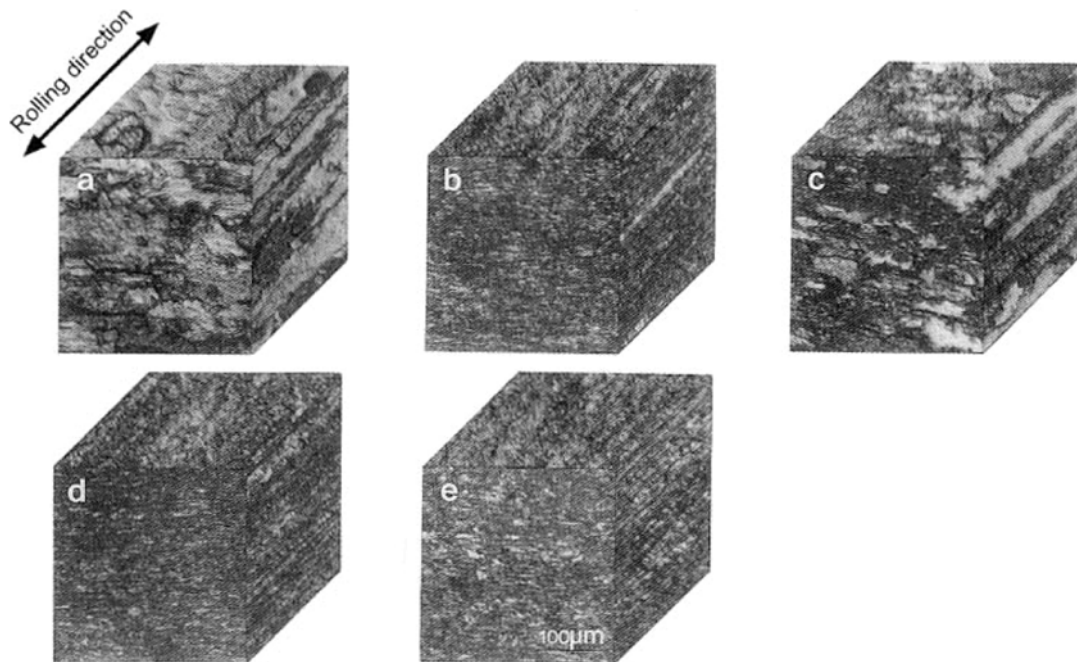


Fig. 5. Three dimensional optical micrographs of the alloys. (a) 17Y-1, (b) 17Y-2, (c) 17Z-1, (d) 17Z-2, and (e) 17M.

and most uniform distribution compared to MgO and ZrO_2 . As shown in Figs. 6 to 10, tensile strength showed a greater effect by grain size connected to the recrystallization of the matrix. We consider that these grain sizes are decided by TMT and annealing heat treatment. Fig. 4 contains the TEM micrographs which show the size and space distribution of the oxide dispersoids in the matrix of the alloys 17Y-1, 17Y-2, 17Z-1, 17Z-2 and 17M. Y_2O_3 particles in the alloys 17Y-1 and 17Y-2 are very fine and are distributed uniformly with a high density. The average particle size of ZrO_2 or MgO is larger and their density less than those of Y_2O_3 . An oxide particle of Y_2O_3 has about a 10-40 nm diameter and particle distribution was shown to be ununiform in the range of $10^{20} \sim 10^{21} m^{-3}$. However, the tensile strength of the alloy 17Z-2 is much greater than that of the alloy 17Y-1. Accordingly, we must consider that the difference of the matrix microstructure in the alloys introduced by the TMT processes also has a very large effect on the strengthening, beyond the effect of the size

and space distribution of the oxide particles.

Optical micrographs of the alloys finally annealed in the TMT process are shown in Fig. 5. The alloys 17Y-1 and 17Z-1 produced by process 1 show large grain growth as indicated in Figs. 5(a) and (c), while such grain growth is not observed in the alloys 17Y-2, 17Z-2 and 17M made by process 2, as indicated in Figs. 5(b), (d) and (e). This large grain growth is considered to be due to the TMT of the hot extrusion and hot rolling performed at a higher temperature than in process 2. TEM observation was made for the analysis of the microstructure in the matrix of the alloys. Figs. 6 to 10 show the analysis results of a recrystallized average grain size shown as high magnification. Figs. 7, 9 and 10 indicate that the very tiny grains (average grain size: about 2 to 4 μm) have a large crystal orientation difference from their neighbouring grains; that is, the matrix of the alloys 17Y-2, 17Z-2 and 17M made by process 2 is composed of very tiny recrystallized grains surrounded by high angle grain boundaries. Here, the reason

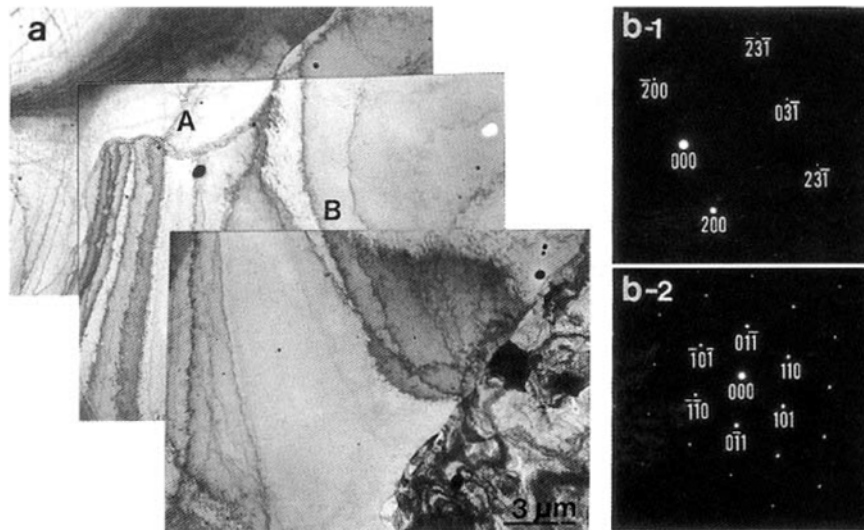


Fig. 6. TEM observation of the matrix microstructure in the alloy 17Y-1. (a) Bright field image, and (b) Selected area diffraction (SAD); b-1: grain A, b-2: grain B.

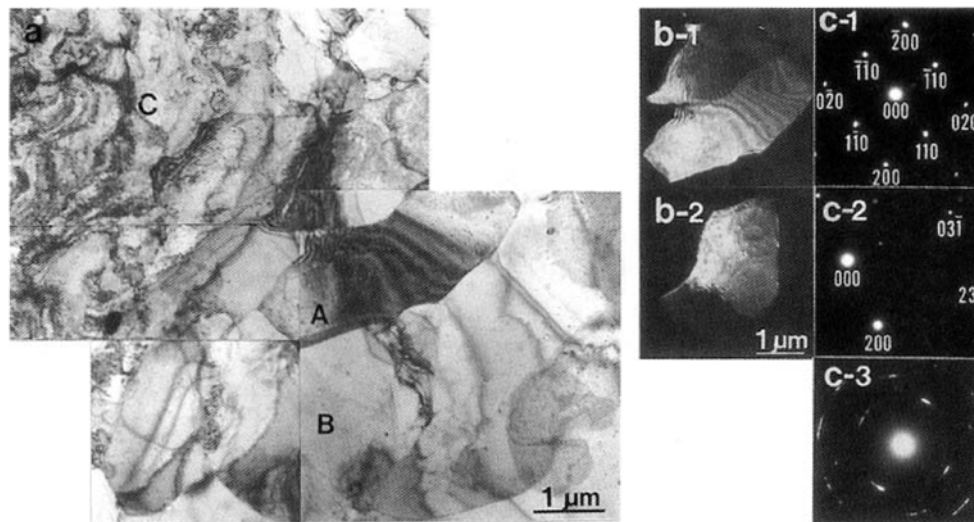


Fig. 7. TEM observation of the matrix microstructure in the alloy 17Y-2. (a) Bright field image, (b) Dark field images; b-1: grain A, b-2: grain B, and (c) Selected area diffraction (SAD); c-1: grain A, c-2: grain B, c-3: area C.

is shown, such as the amorphous ring in the diffraction pattern of Fig. 7 is not a single phase but multi-phase (mixture phase) on a selected area C. On the other hand, Figs. 6 and 8 indicate that the alloys 17Y-1 and 17Z-1 produced by process 1 have very large recrystallized grains (average grain size : about 30 μm) and also have an unrecrystallized region. Here, the difference in recrystallized grain size produced by processes 1 and 2 is due to the temperature difference of hot extrusion and rolling temperature above 200 K after mechanical alloying, and the recrystallization temperature of this alloy actively occurred at above 1400 K. M.A. Miodownik, *et al.* [8] reported that ODS alloys are difficult to recrystallize

as they are the finest and the most uniformly distributed of oxide particles. But the present research showed that strength properties depended more on the TMT temperature after mechanical alloying than the distribution condition of oxide particles. In this TEM diffraction analysis, the specimens are tilted a few degrees (about 2 to 4 degrees) to obtain clear diffraction patterns. Such observation indicates that the TMT process has a significant effect on the microstructural characteristics of the alloys, and that this TMT effect is not affected by the oxide dispersoid species. Accordingly, we can understand that the 17Y-2 alloy having the highest tensile strength is attributed to the combined effect of Y_2O_3 hav-

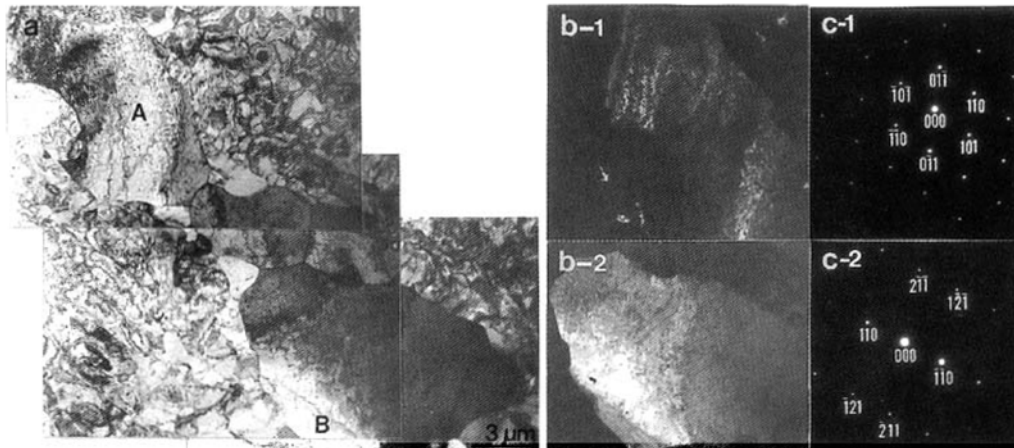


Fig. 8. TEM observation of the matrix microstructure in the alloy 17Z-1. (a) Bright field image. (b) Dark field images; b-1: grain A. b-2: grain B. and (c) Selected area diffraction (SAD); c-1: grain A. c-2: grain B.

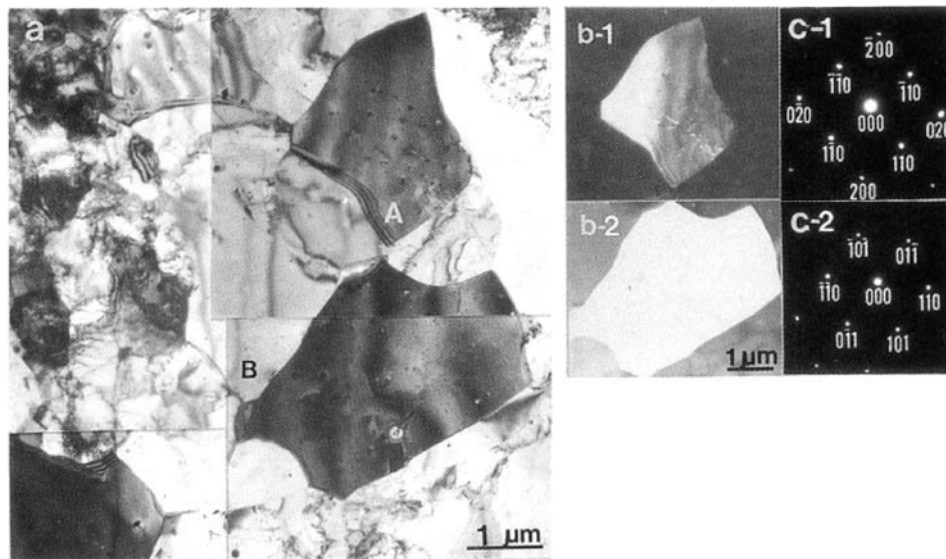


Fig. 9. TEM observation of the matrix microstructure in the alloy 17Z-2. (a) Bright field image. (b) Dark field images; b-1: grain A. b-2: grain B. and (c) Selected area diffraction (SAD); c-1: grain A. c-2: grain B.

ing the finest dispersoid and its uniform space distribution with the highest density, and the matrix microstructure composed of the very tiny recrystallized grains introduced by process 2.

4. CONCLUSIONS

In the present research, the effect of different TMT processes on the strengthening of Fe-17%Cr ferritic ODS-MAs containing Y_2O_3 , ZrO_2 or MgO has been investigated. The following conclusions are obtained.

(1) Y_2O_3 oxide was the finest dispersoid and showed the most uniform space distribution with the highest density in

the matrix among the alloys containing Y_2O_3 , ZrO_2 or MgO .

The alloys containing Y_2O_3 , however, did not necessarily have the largest tensile strength.

(2) The TMT processes had a significant effect on giving the microstructural characteristics of the alloys, and especially process 2 introduced the matrix microstructure composed of very tiny recrystallized grains. This TMT effect was not affected by the oxide dispersoid species.

(3) The largest tensile strength, which the alloy 17Y-2 had, was attributed to the combined effect of the finest dispersoid of Y_2O_3 and its uniform space distribution with the highest density and the matrix microstructure composed of very tiny recrystallized grains.

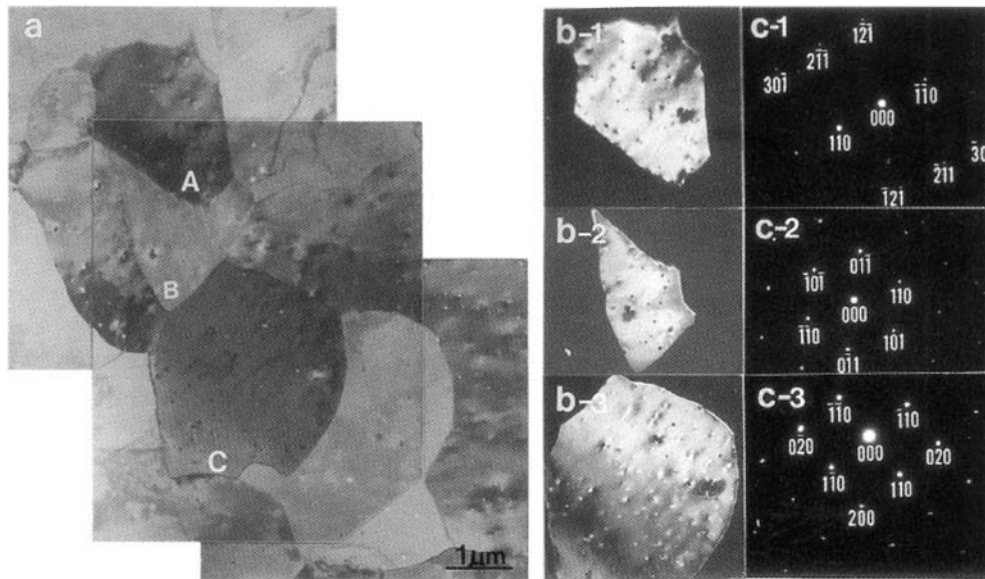


Fig. 10. TEM observation of the matrix microstructure in the alloy 17M. (a) Bright field image, (b) Dark field images; b-1: grain A, b-2: grain B, b-3: grain C, and (c) Selected area diffraction (SAD); c-1: grain A, c-2: grain B, c-3: grain C.

REFERENCES

1. Y. Kawasaki, Y. Ikeda, T. Kobayashi and H. Sumiyoshi, *ISIJ Int.* **36**, 1208 (1996).
2. C.-Y. Kang, M. Fujiwara, D.-S. Bae and K. Miyahara, *ISIJ Int.* **36**, 1518 (1996).
3. I.-S. Kim, C.-Y. Kang, T. Okuda and K. Miyahara, *Proc. of The Third Int'l Symp. on Microstructure and Mechanical Properties of New Engineering Materials* (ed., M. Tokuda), p. 131, Tsu-city, Mie, Japan (1997).
4. S. Ukai, T. Nishida, H. Okuda, T. Okuda, M. Fujiwara, and K. Asabe, *J. of Nucl. Sci. and Tech.* **34**, 256 (1997).
5. E. Orown, *Trans. Inst. Eng. Shipbuild. Scotl.* **11**, 165 (1946).
6. M. F. Ashby, *Z. Metallkd.* **55**, 5 (1964).
7. J. W. Edington, K. N. Melton and C. P. Cutler, *Proc. Mater. Sci.* **21**, 61 (1976).
8. M. A. Miodownik, J. W. Martia and E. A. Little, *Mater. Sci. Tech.* **10**, 102 (1994).